JOURNAL OF GEOPHYSICAL RESEARCH, VOL. 100, NO. C5, PAGES 8571–8586, MAY 15, 1995

Time and space variability in the eastern Alboran Sea from March to May 1990

Álvaro Viúdez[1] and Joaquín Tintoré
Departament de Física, Universitat de les Illes Balears, Palma de Mallorca, Spain

Abstract. An intensive field experiment was carried out from March 6 to April 30, 1990, in the eastern Alboran Sea to understand the relationship between the large-scale circulation and the location of the transition zone between new and longer-resident Modified Atlantic Water (MAW). The detection of a strong jet (80 cm s^{-1}) of new MAW with anticyclonic curvature near the Morocco coast suggests that the Eastern Alboran Gyre (EAG) was not fully developed. A new state of the circulation in the eastern Alboran basin, intermediate between the EAG (Viúdez et al., 1995) and the Lanoix (1974) state, is presented. Also important is that the Almería-Oran Front was not present in the upper layer, that small-scale instabilities were detected in the northern region, and that significant nongeostrophic flows were observed. All these features are clearly indicative of the high spatial and temporal variability of a region where complex adjustments among density, velocity, and topography occur.

1. Introduction

The Alboran Sea is the first Mediterranean basin encountered by the Modified Atlantic Water (MAW), ($36.5 < S < 37.5$, where S is salinity and values are practical salinity units). Recent international experiments such as Donde Va? in 1982 [*Donde Va? Group*, 1984] and the Western Mediterranean Circulation Experiment in 1986 [*La Violette*, 1990] have shown that the circulation of MAW in the Alboran Sea is characterized by high spatial and temporal variability. The large-scale circulation is fairly well known and shows that at any one time there are one or two large anticyclonic gyres, one lying in the western Alboran basin (the Western Alboran Gyre) and the other in the eastern Alboran basin (the Eastern Alboran Gyre (EAG)). Typical dimensions for the diameter of theses gyres are around 100 km, while the internal Rossby radius in the Alboran Sea is ~20 km [*Gascard and Richez*, 1985].

Several studies in the Alboran Sea have addressed the problem of the variability of the MAW in the western basin. In situ studies have shown significant mesoscale nonnegligible temporal variability [*Perkins et al.*, 1990; *Heburn and La Violette*, 1990]. Most of the numerical studies examined the question of the anticyclonic gyre formation and indicated that the existence of the western gyre might be related to the nonlinear density advection off the Strait of Gibraltar [*Wang*, 1987]. While most of these studies were carried out to understand the dynamics of the western Alboran basin and its relation to the strait's outflow, much less information exists on the dynamics of the eastern basin, east of Cape Tres Forcas. The few data available indicate that several circulation patterns are possible. *Lanoix* [1974] found an eastward current with positive vorticity in the south of the eastern basin near the Morocco coast. *Heburn and La Violette* [1990], in an intensive study of the temporal variability using satellite imagery, showed that large variations in the surface signature of the two gyres occur and that one or the other gyre can actually disappear. *Viúdez et al.*, [1995] found, in the entire Alboran, a wavelike front coupled with two anticyclonic gyre-cyclonic eddy systems.

The eastern boundary of the EAG (when present) forms sometimes a well-defined feature called the Almería-Oran Front [*Tintoré et al.*, 1988]. This front results from the convergence, south of Cape Gata, of new MAW and longer-resident (and more saline, S>37.5) MAW. *Tintoré et al.* [1988] described this very intense density front as limited to the upper 300 m and with an associated southeastward baroclinic current (50-100 cm s^{-1}). Part of this flow continues eastward and initiates the Algerian Current, confined to the upper 150 m and characterized by a transport of $0.4 - 0.5$ Sv [*Arnone et al.*, 1990]. In summary, these studies in the eastern Alboran basin show that two very different circulation patterns are generally found, one associated with the existence of the EAG, and sometimes the Almería-Oran Front, and the other with no gyre and a pronounced eastward flow at Cape Tres Forcas [see *Heburn and La Violette*, 1990, Figures 1 and 2].

[1]Now at Department of Meteorology, Naval Postgraduate School, Monterey, California.

Paper number 94JC03129.
0148-0227/95/94JC-03129$05.00

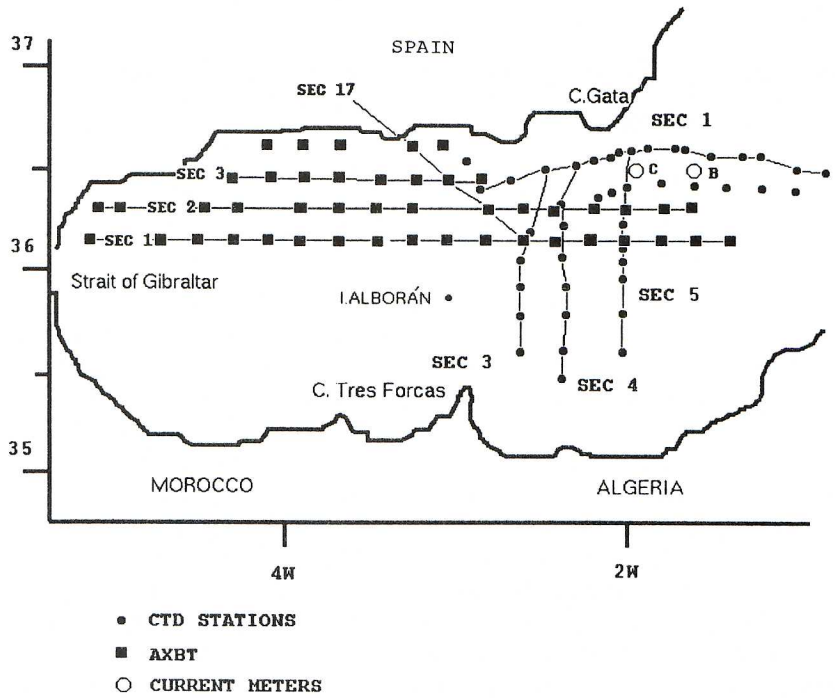

Figure 1. The Alboran Sea. Conductivity-temperature-depth (CTD) profiler, airborne-dropped expendable bathythermograph (AXBT) locations, and current meter moorings are provided. The different vertical sections are referenced.

However, even after all these international programs, several questions still remain without answers. In particular, the physical mechanism responsible for the collapse of the EAG, the relationship between the gyre and the Almería-Oran density Front, and the importance of mesoscale dynamics in the eastern Alboran are still unknown. The goal of this paper is to address these questions. The work is organized as follows: in section 2 we briefly present the data collected during an intensive study carried out from March to May 1990. Owing to the amount of data available, we identify several important topics that are described in section 3. In particular, we describe the large-scale structures as observed from March 6 to 15, the physical characteristics of the eastward jet found in the southern region and its biochemical implications, and also describe the northward

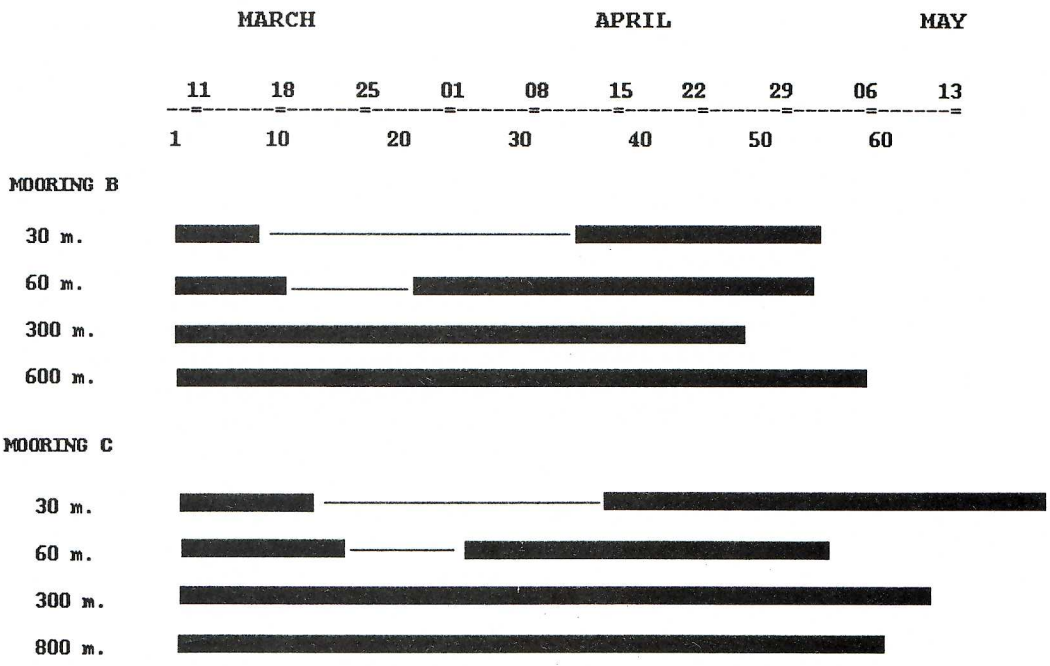

Figure 2. Data-recorded periods of the current meters.

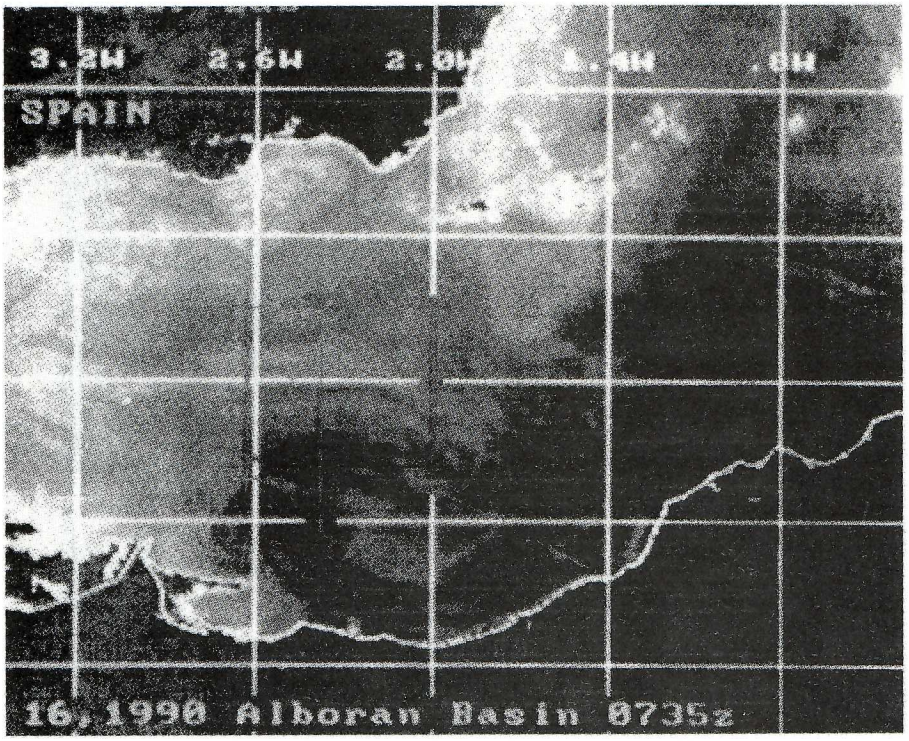

Figure 3. Satellite thermal imagery for March 16, 1990. Darker shades represent warmer water.

jet found in the northeastern Alboran. In the section 4, emphasis is made on the characterization of an intermediate state of the circulation and on the importance of mesoscale variability as inferred from comparison between acoustic Doppler current profiler (ADCP) and geostrophic velocities. Finally, a sketch of the circulation pattern described in this study is presented and discussed.

2. Data

The field experiment was carried out from March 6 to April 30, 1990. An extensive data set from different sources, including airborne-dropped expendable bathytermograph (AXBT), conductivity-temperature-depth (CTD), ADCP, and current meters was obtained. In this section we briefly present the different phases of this field experiment.

On March 9 a 6-hour flight was carried out on a search and rescue (SAR) instrumented aircraft at an altitude of 600 feet (182.9 m) and a speed of 120 knots (222 km h^{-1}). The aircraft was equipped with an RF receiver, and data were continuously received onboard. Sippican AN/SSQ-36 AXBTs were dropped every 10 miles (16 km). Temperature accuracy, as indicated by the manufacturer is ± 0.2°C , depth accuracy is $\pm 2\%$. Radio frequency interference caused bad reception for those AXBTs dropped near the coast (shallow waters) and resulted in 46 successful drops (Figure 1). Bad weather conditions did not allow samplings to be made in the southern Alboran Sea.

Satellite images for the period March 1 through April 30 have been also analyzed. Four National Oceanic and Atmospheric Administration (NOAA) 10 advanced very high resolution radiometer (AVHRR) images were selected from a set of approximately 16 scenes of the Alboran basin. These are AVHRR scenes (channel 4) and represent relative sea surface temperature, where the darker shades represent warmer water. All image processing was performed using the NASA developed Sea Pack image processing system [*McClain et al.*, 1992].

The region south of Cape Gata was sampled onboard the R/V *García del Cid* from March 6 to 15 using a Neil Brown CTD. Vertical casts (Figure 1) were made at 49 stations to determine the vertical structure. Distance between stations was usually around 10 miles (16 km) except in a west-east cross section, south of Cape Gata, where more intense sampling was made. In addition, continuous surface temperature and salinity were also recorded. Horizontal components of velocity were continuously monitored using a ship-mounted ADCP with vertical resolution of 8 m and a maximum depth of 300 m. Five-minute averages were carried out, implying a horizontal resolution of 1.5 km. At every station the continuous monitoring was interrupted and ADCP data were then collected while the ship remained stationary.

Finally, two moorings with four Aanderaa current meters each were anchored south of Cape Gata at site B (36°31.35' N; 1°37.79' W) and site C (36°32.79' N; 2°01.96' W), from March 9 to May 15 (Figure 1). The first mooring (B) was deployed over a submarine ridge at a depth of 760 m with current meters placed at 30, 60, 300, and 600 m. The second (mooring C), located 30 km away, was deployed at a depth of 1100 m, with current meters placed at 30, 60, 300, and 800 m. Sampling period was set to 30 min. Figure 2 shows the data obtained for the two moorings at the different depths.

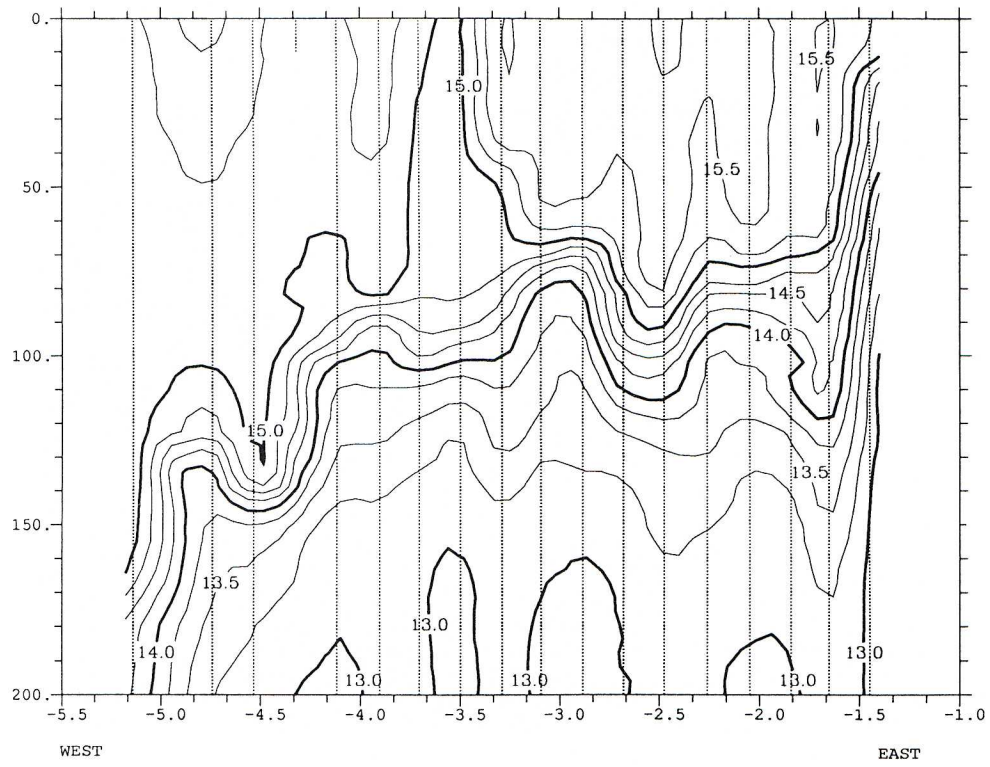

Figure 4. West-east temperature distribution from AXBT data (vertical section A1).

3. Results

In this section we initially present the large-scale structures detected using satellite imagery, AXBT, and CTD data. Next, we study the smaller-scale structures detected in the southern and northern Alboran Sea as obtained from CTD and ADCP data and examine their biological effects. Finally, we present the results obtained from the two current meter moorings.

3.1. Large-Scale Structures

Satellite imagery for March 16 (Figure 3), presented at the full resolution of the satellite sensor and in a Mercator projection, indicate that in all the Alboran Sea the horizontal surface temperature gradients were weak. However, northeast of Cape Tres Forcas, a well-defined gyre/filament was detected. Surface temperature and salinity obtained from CTD and AXBT data were in the range of 15–16°C and 36.4–36.9 psu. Figure 4 shows that below the layer of new MAW, a well-defined vertical temperature gradient, ~40 m thick, was observed. This interface between new and older MAW was also detected in the southern region characterized by strong temperature and salinity vertical gradients (15.00–14.00°C ; 37.2–38.0 psu). Two regions with large horizontal temperature gradients can be also observed (Figure 4) near the Strait of Gibraltar, where the most abrupt adjustment takes place, and south of Cape Gata, where the Almería-Oran Front had been observed in previous studies [*Tintoré et al.*, 1988; *Arnone et al.*, 1990].

3.2. Eastward Jet in the Southern Alboran

Northeast of Cape Tres Forcas, a well-defined front was detected below 30 m. Since temperature and salinity effects are additive, we only show the resultant density field (Figure 5a). The vertical density σ_t distribution shows that this front was found from 30 to 200 m and was characterized by a width of the order of 37 km (20 miles). The stronger density gradients were found between 100 and 200 m (1 σ_t unit in a horizontal distance of 18 km) and were also found at similar latitudes in vertical sections 3 and 5, but 10 km northward in vertical section 4. This northward shift is also visible in Figure 3 and is confirmed by independent ADCP data. Note the doming of isopycnals observed near 36°N between 50 and 100 m (Figure 5a) indicative of strong horizontal shears. This doming was not observed in the other two north-south vertical sections (vertical section 4 in Figure 6a and section 5, very similar to section 4, not shown). The ADCP eastward velocity component associated with this density gradient (Figures 5b and 6b) was strong, reaching values of 80 cm s^{-1} at 20-30 m. Transport computations showed the total eastward integrated current was high, of the order of 2.4 Sv for vertical section 3, and 2.8 Sv for vertical section 4. As indicated above for the density gradients, the core of the eastward jet (at 20-30 m, 60-80 cm s^{-1}) was observed at different latitudes in vertical sections 3, 4, and 5. The north-south components of the core of the jet were 20, 0, and (-40) cm s^{-1} in vertical sections 3, 4, and 5, respectively (Figures 5c and 6c), and as a result, the jet had antyciclonic curvature (see also the

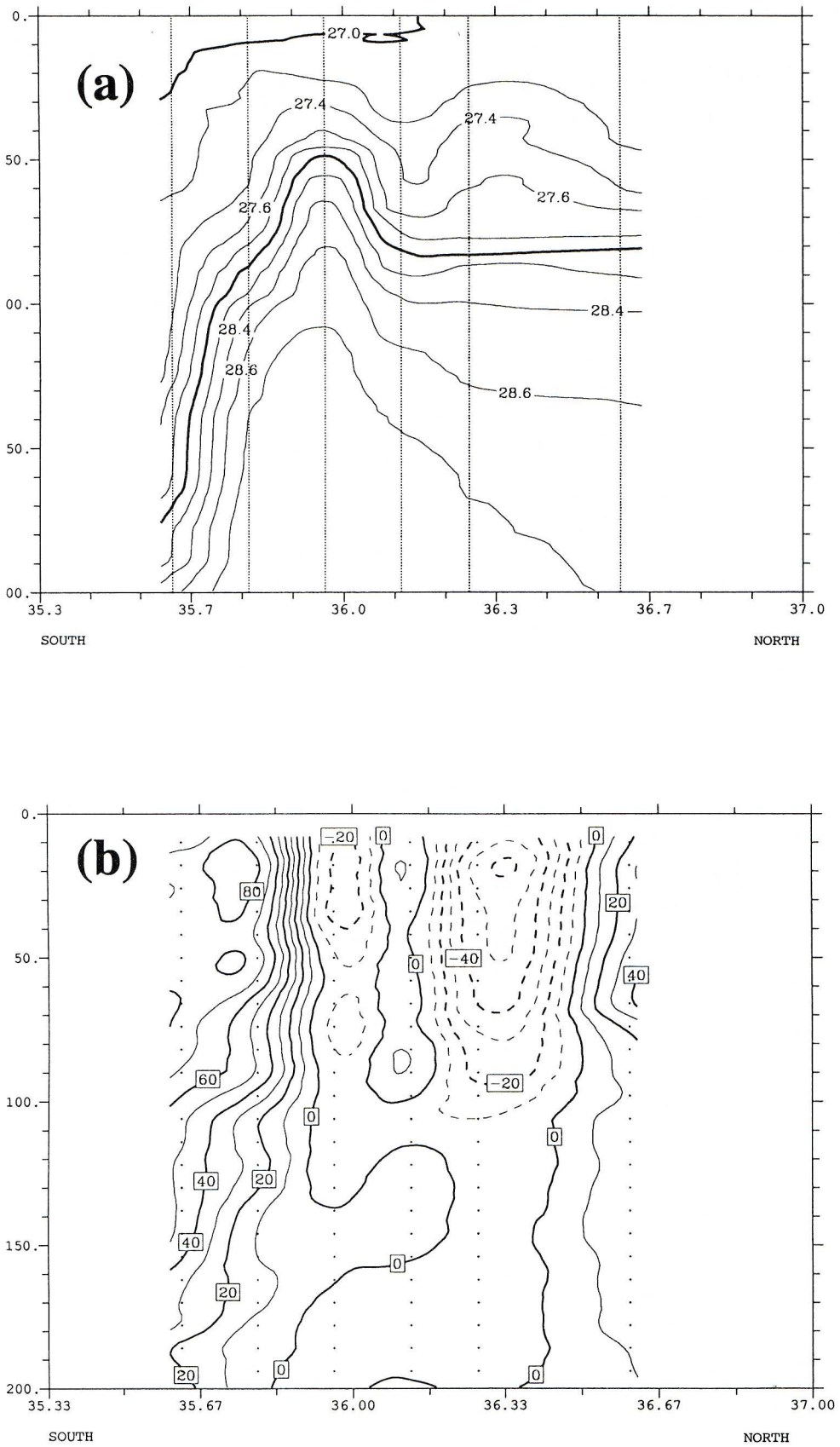

Figure 5. South-north vertical distribution in vertical section 3 showing (a) density σ_t, (b) east-west acoustic Doppler current profiler (ADCP) component (continuous contour line means eastward direction), (c) north-south ADCP component (continuous contour line means northward direction), (d) SiO_2, and (e) chlorophyll.

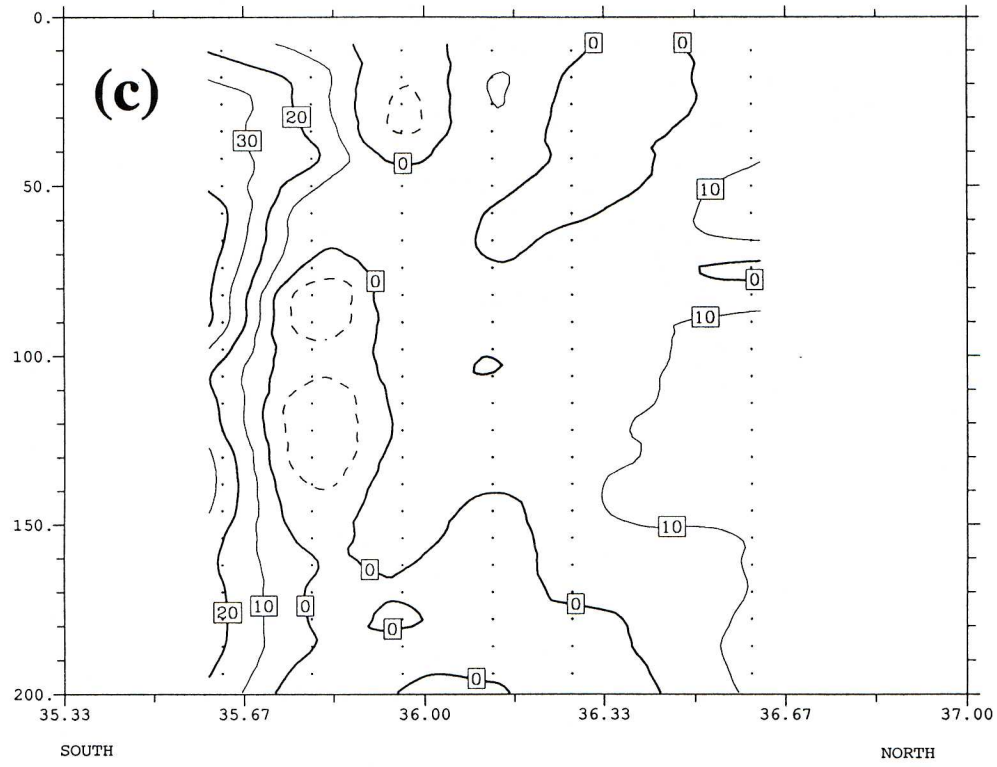

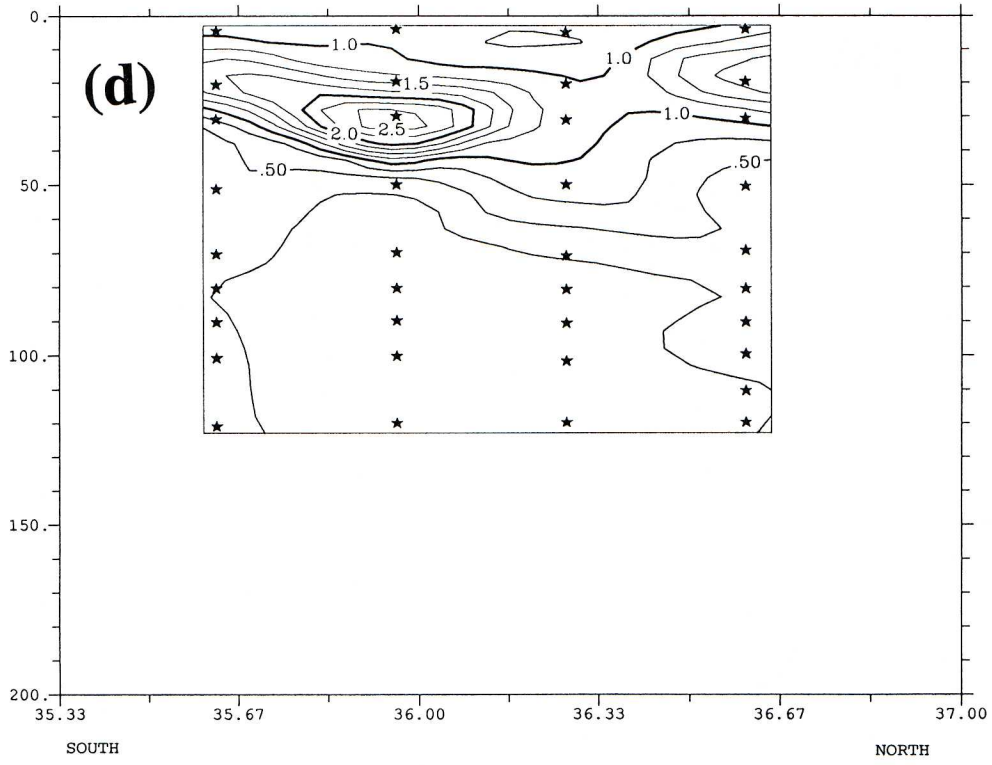

Figure 5. (continued)

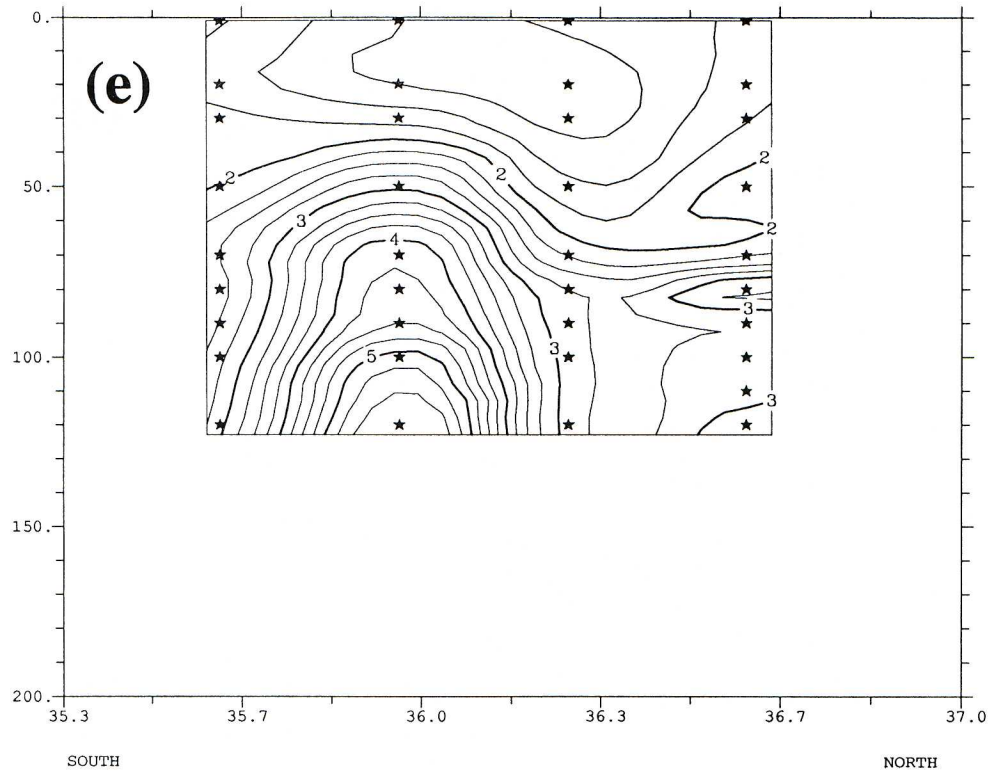

Figure 5. (continued)

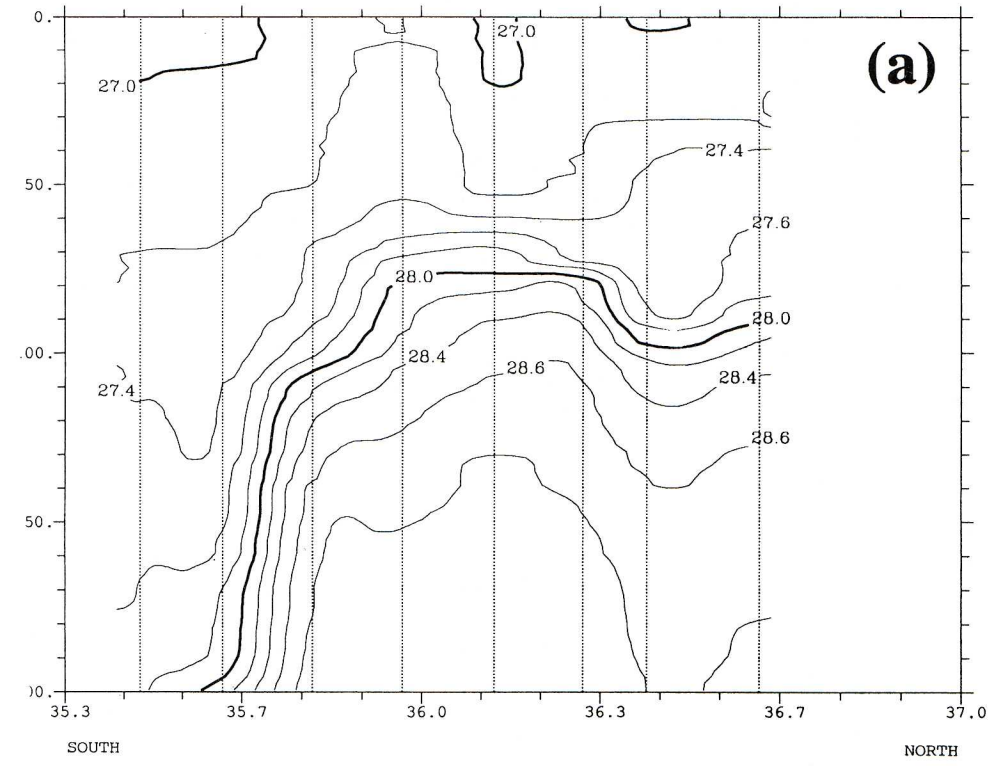

Figure 6. South-north vertical distribution in vertical section 4 CTD showing (a) $sigma_t$, (b) east-west ADCP component (continuous contour line means eastward direction), and (c) north-south ADCP component (continuous contour line means northward direction).

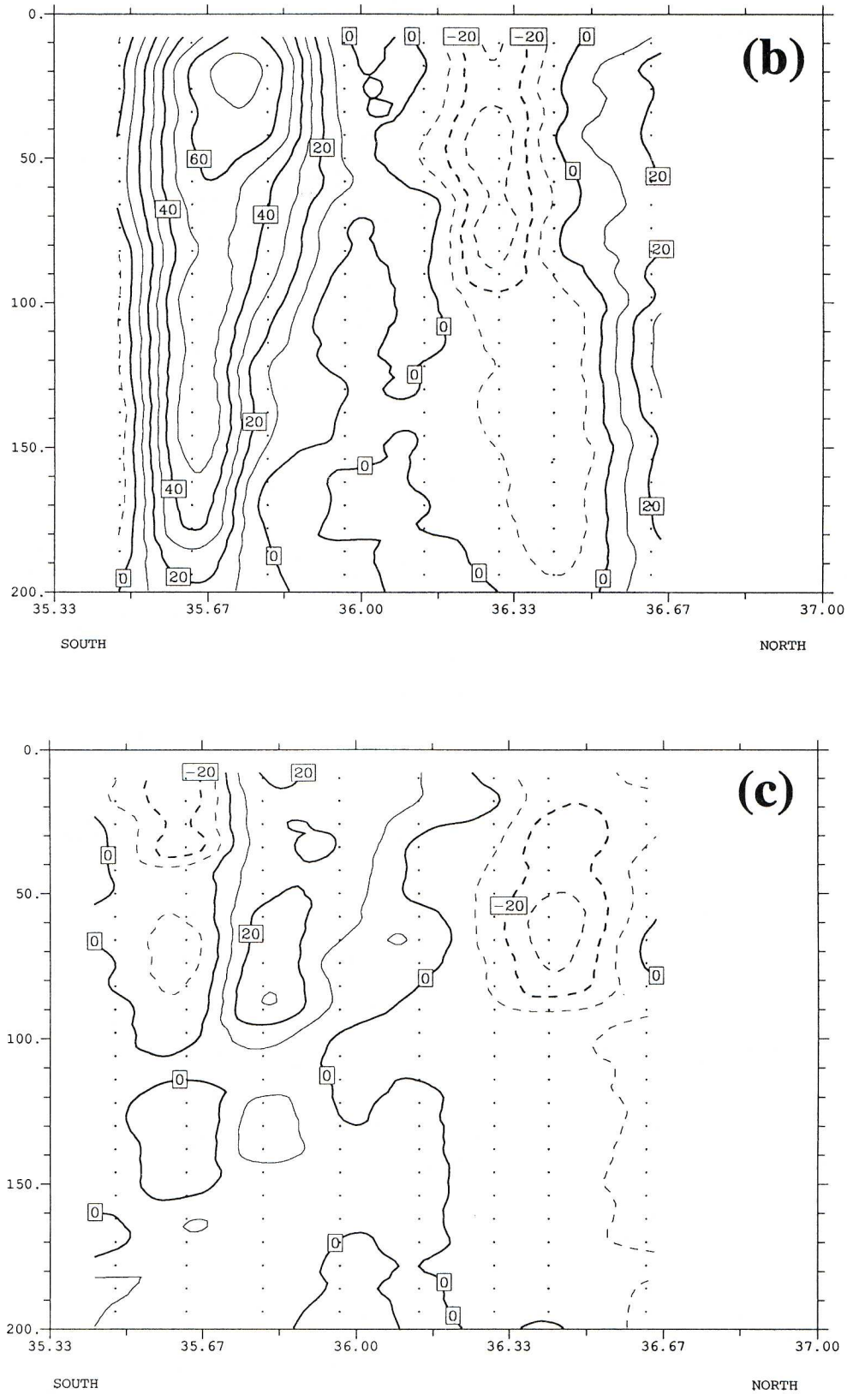

Figure 6. (continued)

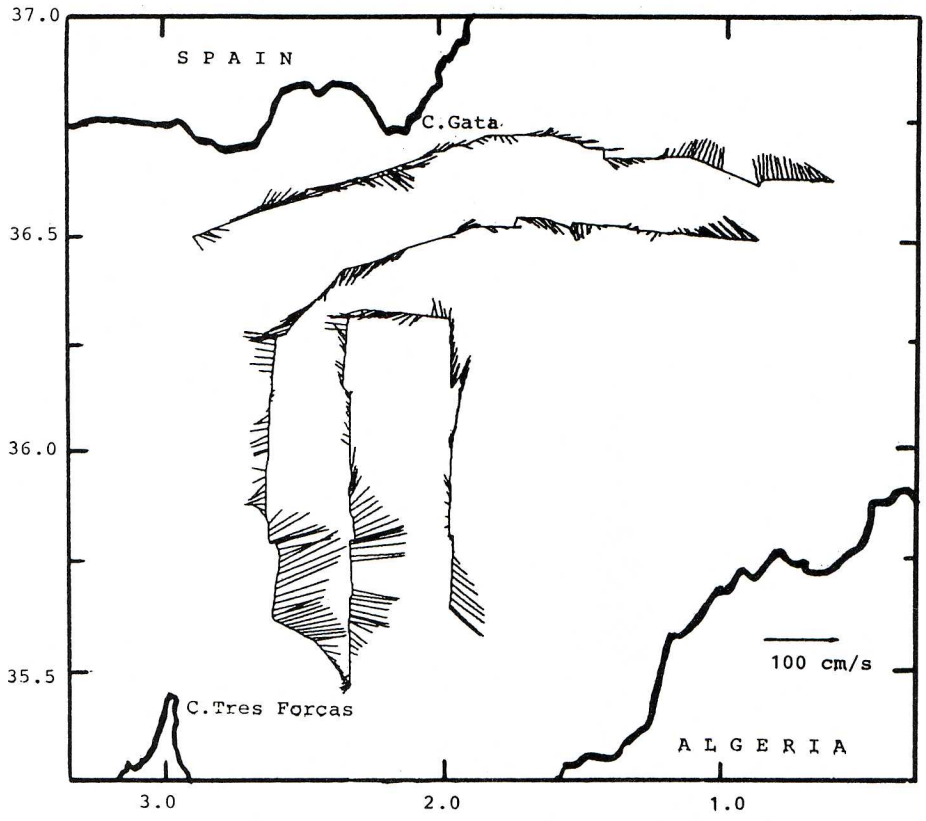

Figure 7. Horizontal distribution of ADCP data at 10 m.

horizontal distribution of ADCP data, Figure 7). The surface signature of this jet can now be traced in Figure 3 that shows a circular gyre/filament of warm water developing in the southern region whose northern part coincides with the surface location of this jet.

Given the significance of this well-defined eastward jet, we have tried to establish its biological and chemical effects. The distributions of SiO_2 (Figure 5d) and NO_3 (not shown) show a dome located north of the jet (36°N) and suggest that upward water advection occurred on the northern side of the jet. Accordingly, the chlorophyll distribution for vertical section 3 (Figure 5e) showed maxima in the same location.

3.3. Northward Jet in the Northeastern Alboran

The vertical distributions of temperature, salinity, and density for CTD vertical section 1 are shown in Figures 8a, 8b and 8c. The vertical distribution of σ_t (Figure 8c) shows significant density gradients present from the surface down to 150 m. A similar feature was observed in vertical section 2 (not shown). The largest gradient was located at 100 m (0.5 σ_t in 18 km), while at the surface the horizontal temperature range was smaller than 0.75°C (Figure 8a). The satellite imagery (Figure 3) shows a boundary region between warm and cold water, at 1°1'W and 36°40'N, that coincides with the western limit of this northward jet. The analysis of the ADCP data in vertical sections 1 and 2 also shows the existence of this northward jet, whose north-south velocity component is shown in Figure 8d. The entire jet occupied the first 110 m, with a horizontal northward transport of ~1.6 Sv. The core (maximum velocities of 50 cm s^{-1}) was located at 0°40'W between 20 and 30 m.

3.4. Current Meter Results

Current meter data were analyzed to investigate the magnitude of high- and low-frequency motions. Low-frequency currents were obtained using a low-pass complex filter with a cutoff period of 33 hours. The residual current at 30 and 60 m had a mean value of 10 cm s^{-1} to the southeast (note that this is approximately the same direction as the expected current associated with the Almería-Oran Front). No significant differences were found in the low-frequency currents at 30 and 60 m on both moorings B and C. However, an exception was found in the last part of the recorded period (from April 17 to the end). During this period, moorings B30 and B60 indicate a progressive rotation from southeast to northeast, with an associated amplitude increase reaching 35 cm s^{-1} (Figure 9a). This surface current modification was associated with a temperature increase and a salinity decrease, suggesting the presence of new MAW. At 300 and 600/800 m the residual current was only 1-2 cm s^{-1} without dominant direction (not shown). At higher frequencies we found strong inertial

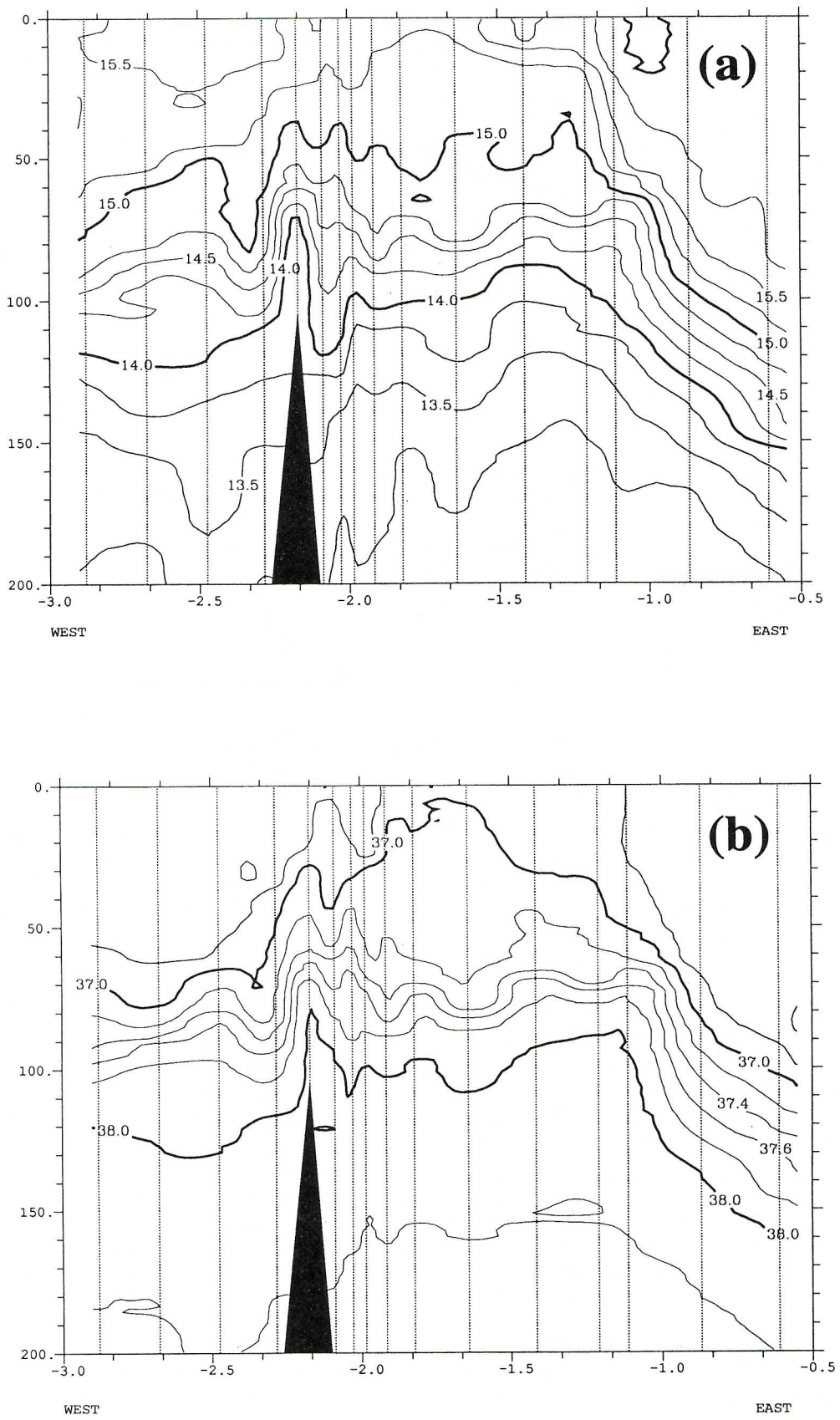

Figure 8. West-east vertical distribution in vertical section 1 CTD showing (a) temperature, (b) salinity, (c) σ_t, and (d) north-south ADCP component (continuous contour line means northward direction).

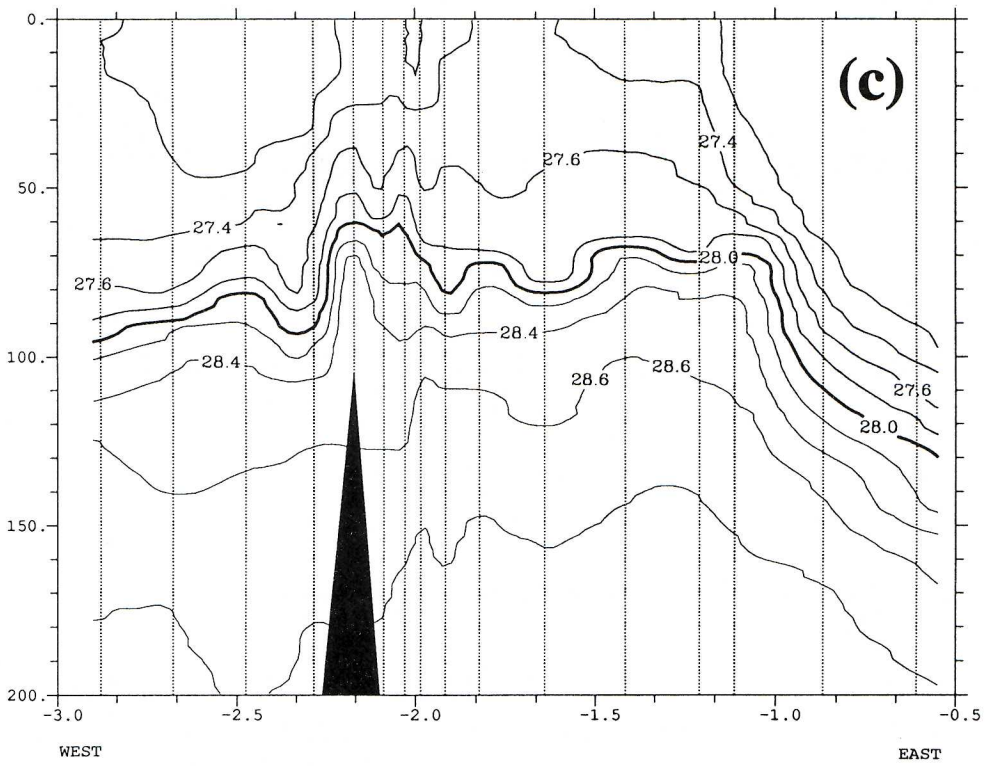

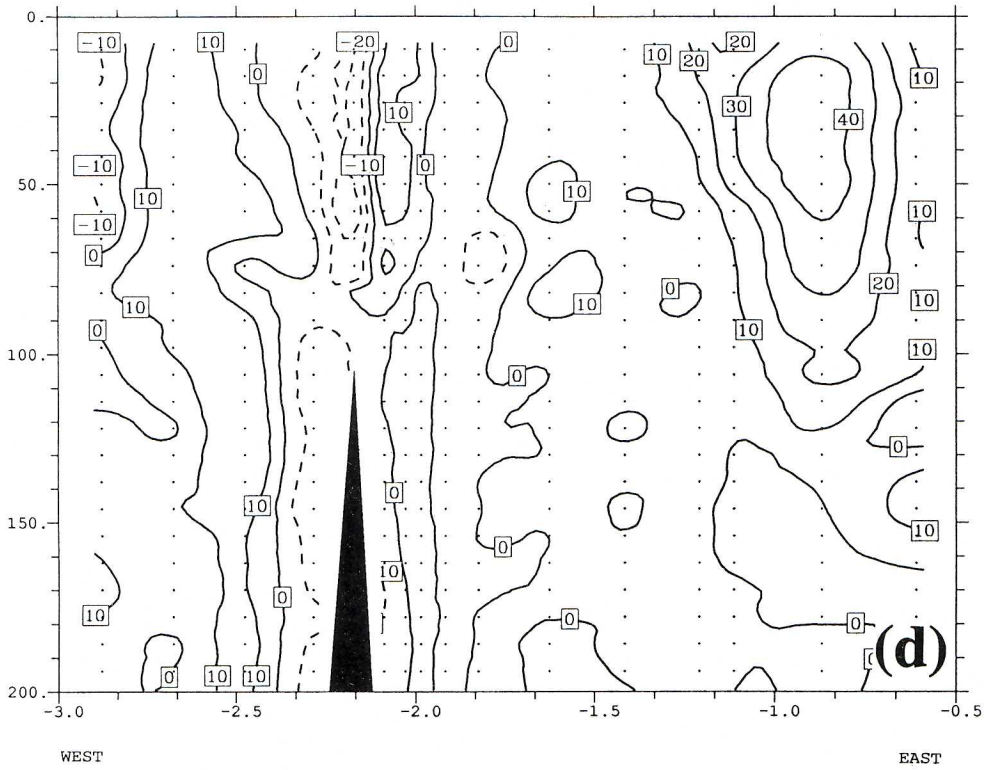

Figure 8. (continued)

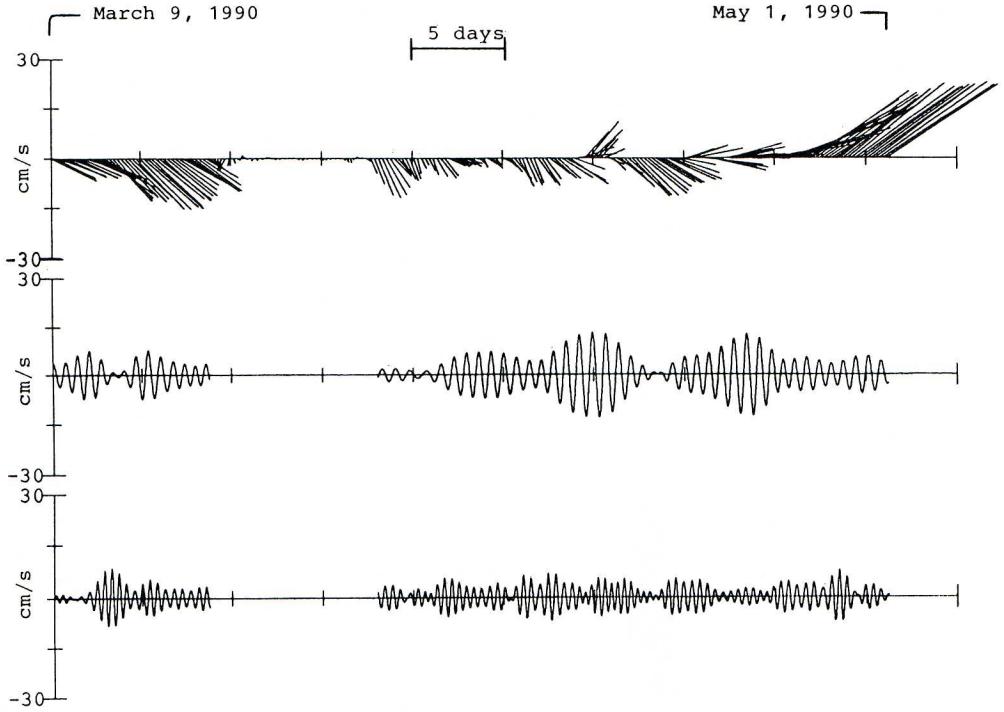

Figure 9. Time series of B60 current meter (60 m). (a) Stick diagram of the low-pass (33 hours) filtered, (b) inertial component (U component), and (c) tidal (semidiurnal) component (U component).

components (with maximum amplitudes of 30 cm s^{-1}) in the upper layer (30, 60 m, Figure 9b). This high-frequency component of the velocity should be carefully analyzed and taken into account before detailed analysis of ADCP data in the Alboran Sea is made. The inertial component at 300 and 600 m was smaller, though still significant (5–10 cm s^{-1}). Inertial amplitudes decayed in a few days. Also, it is important to note that a small tidal component (semidiurnal, Figure 9c) was detected with 10 cm s^{-1} amplitude at 30–60 m and about 5-10 cm s^{-1} at 300-600 m.

3.5. Geostrophic Computations

Geostrophic velocities were computed using 300 m as the reference level, similar to the reference level taken with the ADCP (i.e., the ADCP data at any point are the deviation from the mean ADCP value around 300 m). This choice allowed us to compare the geostrophic and ADCP currents. Figure 10a shows that the eastward jet previously described was approximately in geostrophic balance. The slight differences can be explained by the discrete sampling showed here (continuous ADCP data (Figure 7) actually describe in detail the core of the jet, with maximum values for the east component of ~100 cm s^{-1} in vertical section 3 and 90 cm s^{-1} in section 4). An important difference was found at middepth (50 m), where the ADCP data indicated maximum velocities, while geostrophic computations showed maximum velocities at the surface. North of the jet, the westward geostrophic current reached maximum values of 50 cm s^{-1}, significantly higher than the 20 cm s^{-1} ADCP values. Differences between ADCP and geostrophic computations also exist in vertical section 3, near 36°20' N. These differences are clearly high (larger that the expected maximum magnitude of inertial waves at this depth) and suggest the existence of transient adjustment processes, likely associated with mesoscale variability. On the other hand, in vertical section 4 the same westward current (Figure 6b, 30 cm s^{-1} core) extends down to 200 m and is comparable to the geostrophic computations shown in Figure 10b. The northward current observed in Figure 8d was also mainly geostrophic.

4. Discussion

Our analyses of in situ data collected in March 1990 describe the existence of a strong eastward jet with anticyclonic curvature as the main feature present in the eastern region. In this section we discuss the results presented and suggest that this new circulation pattern (not previously described using "in situ" data) was actually a transition state, intermediate between the fully developed EAG [*Viúdez et al.*, 1995] and the *Lanoix* [1974] state.

In all the region sampled the upper layer was occupied by new MAW (with salinities between 36.4 and 36.9). This is fairly different from previous studies, where more saline waters (~37.8) were found west of the Almería-Oran Front [*Tintoré et al.*, 1988; *Arnone et al.*, 1990]. In our study the two current meter moorings (B and C) and several CTD and AXBT stations

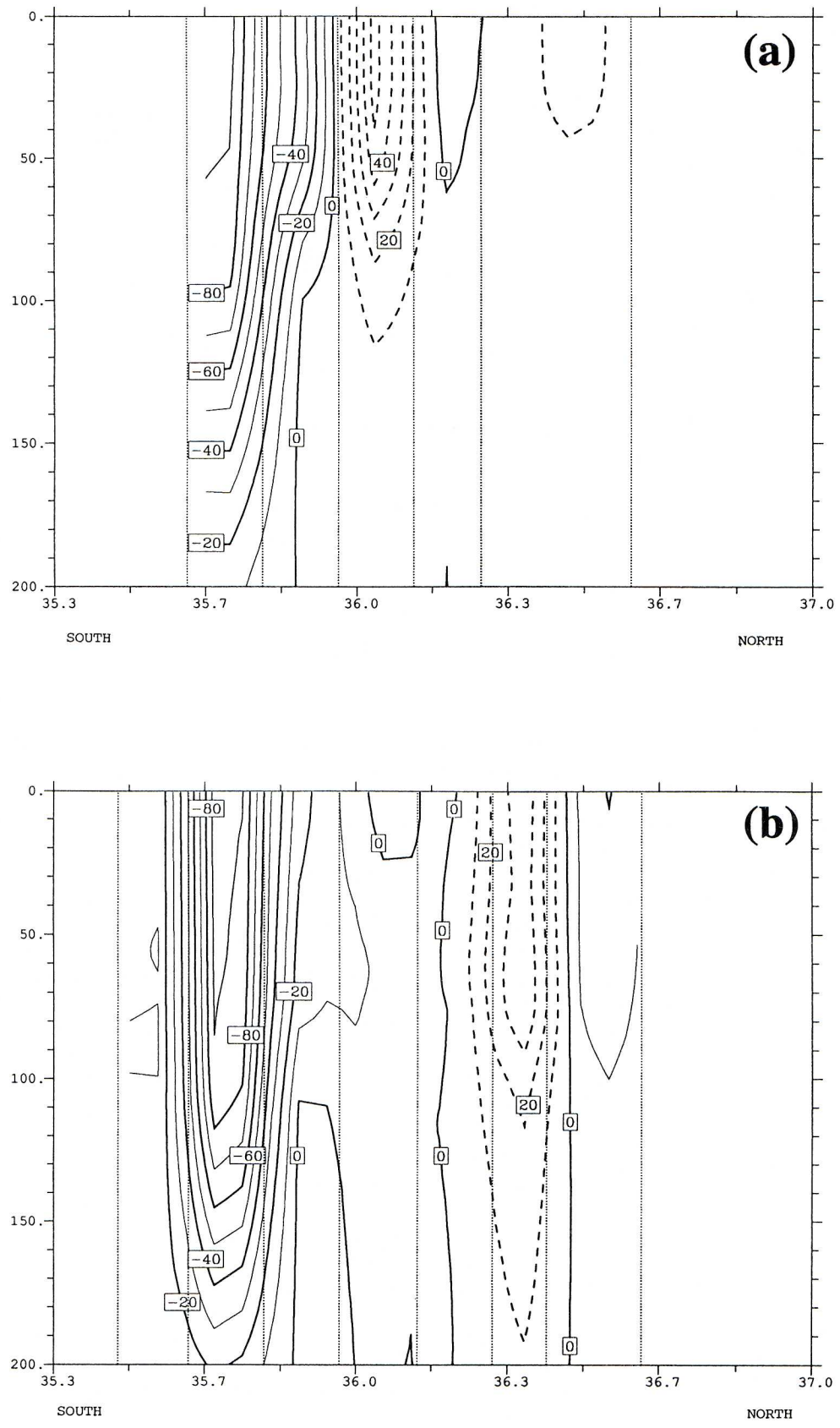

Figure 10. East-west geostrophic velocity for (a) vertical section 3 CTD and (b) vertical section 4 (continuous contour line means eastward direction).

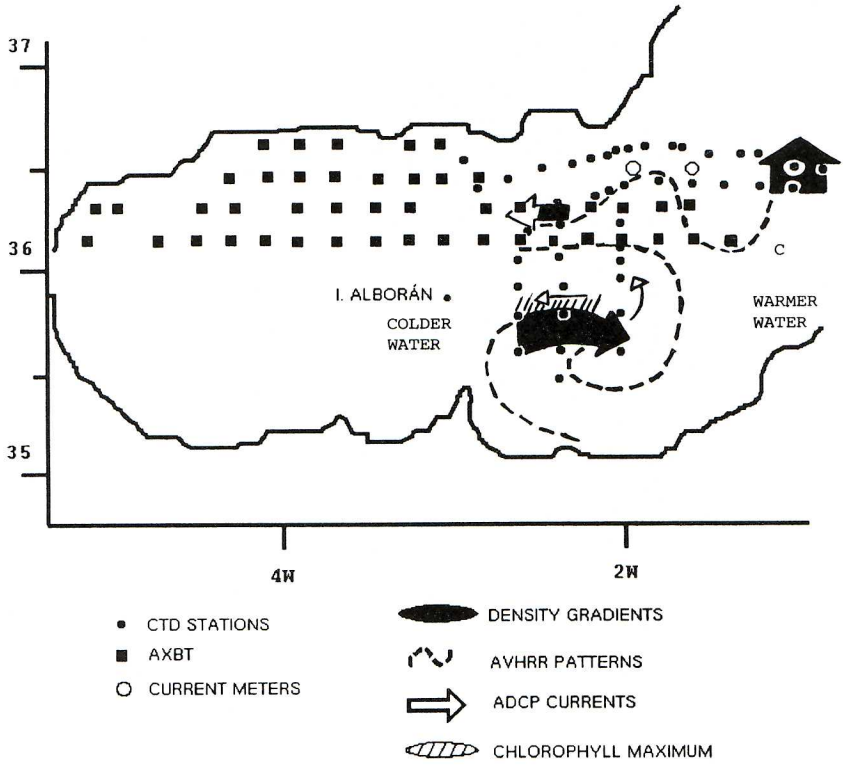

Figure 11. Upper layer circulation pattern.

(i.e., between 1°–2° W and 36°–36°40'N) made in the area where the Almería-Oran Front had been previously reported did not show clear evidence of the front in the upper layer. Neither a fully developed gyre/front structure nor an eastward jet with positive vorticity near the Morocco coast was present. Instead, we found a well-defined eastward jet with anticyclonic curvature in the southern region. This eastward jet is similar to the one described by *Lanoix* [1974] except that the one described here has anticyclonic curvature. This difference and the presence of a circular pattern in the satellite thermal image (whose northern part coincides geographically with the jet, Figure 3) suggest that the state of the circulation in the eastern Alboran basin in March 1990 was an intermediate state where the EAG was not fully developed and that, instead, a smaller anticyclonic gyre was observed in the southern part of the eastern Alboran basin. A sketch of the new circulation pattern in the upper layer (~50 m) is shown in Figure 11. This state would correspond to the satellite image of July 7, 1982, in the history of the gradual redevelopment of the EAG [*Heburn and La Violette* 1990]. The hypothesis that this jet is part of a small anticyclonic gyre is strongly reinforced by transport values. The jet has a transport of about 2.8 Sv, a value higher than previously reported computations for the Algerian Current. For example, *Arnone et al.* [1990] found only 0.4–0.5 Sv at 3° E in May-June 1986, similar to the geostrophic transport computed by *Perkins and Pistek* [1990]. The total eastward transport in the eastern Alboran basin when the EAG was well developed in Octuber 1992 was 2.2 Sv, with 1.2 Sv associated with the gyre and the other 1 Sv with the wavelike front [*Viúdez et al.*, 1995]. The high value of 2.8 Sv found in March 1990 also suggests the existence of a splitting of the flow that recirculates, closing the EAG, and that also forms, eastward of the gyre, the origin of the Algerian Current [*Heburn and La Violette*, 1990; *Viúdez et al.*, 1995].

The latitude of the two current meters moorings (~36° 30'N) marks the northern boundary of the Almería-Oran Front when observed. At the beginning of the study period both current meters were clearly westward of the northward jet described in Figure 8d. As a result, the shift in current meter data observed only at moorings B suggests that the northward jet had shifted its initial location to a more westward location. A northeastward current along Cape Gata is frequently observed from satellite imagery when the EAG is present [*Heburn and La Violette*, 1990; *Viúdez et al.*, 1995]. Thus the progressive increase of a northeast current measured in the upper current meters might be associated with the formation of the EAG, therefore reinforcing the idea that the March 1990 state was a transient state. Further support for this evolving situation is given by the differences between ADCP and geostrophic velocities. While geostrophic computations, in general, agree with ADCP data in the eastward (except in the upper 50 m) and northward jet, the presence of important deviations from geostrophy (larger than the expected magnitude of inertial waves) found mainly in the middle of the eastern Alboran basin is indicative of the rapidly changing state of the circulation.

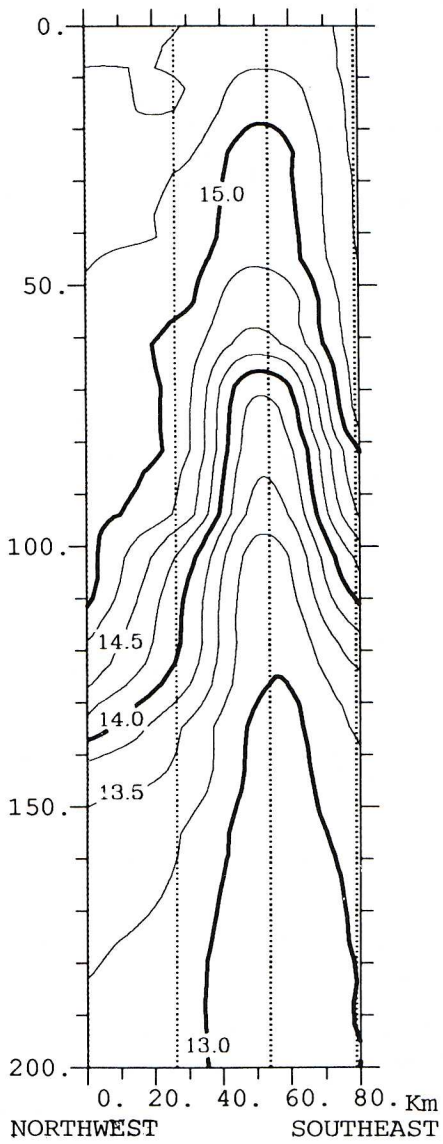

Figure 12. Temperature distribution in the AXBT vertical section A17.

The second important point to be discussed on a global frame is the importance of mesoscale features. The domes observed from the AXBT data in the northern Alboran basin, near the Spanish coast, reveal the significant mesoscale variability of this region. For example, Figure 4 shows that rising of the new/older MAW interface (between the 14 and 15°C isotherms) occurs at 36° 20'N, between 3° 30'W and 2° 40'W. This feature is better observed in a northwest–southeast vertical section (section A17 AXBT, Figure 12), where the entire temperature field between 14 and 15°C forms a well-defined dome. The depth of the 14.5°C isotherm (Figure 13) shows a circular structure that corresponds to a cyclonic eddy. The dynamic effects on the vertical velocity of mesoscale cyclonic eddies found along the boundary of the large-scale Western Alboran Gyre have been studied by *Tintoré et al.* [1991] and *Viúdez et al.* [1995]. *Tintoré et al.* [1991] found that the vertical motion associated with these mesoscale eddies was an order of magnitude higher than the large-scale vertical motion. Unstable filamentary features of the Almería-Oran Front have been also recently observed from remote sensing observations [*Davies et al.*, 1993], showing that these filaments have length scales comparable to the front itself, growing and decaying on a timescale of a few days.

In summary, we have described physical and biological observations of the eastern Alboran basin that characterize a transient state of the circulation, intermediate between the fully developed EAG [*Viúdez et al.*, 1995] and the *Lanoix* [1974] pattern. Although the importance of mesoscale structures in the adjustment process has been addressed, their influence on the large scale circulation is still unknown, as is the case of other Mediterranean subbasins [e.g., *La Violette*, 1994]. Further studies are needed to clarify the EAG formation (large scale), its relation to the Almería-Oran Front, and the quantitative importance of mesoscale eddies in the Alboran Sea.

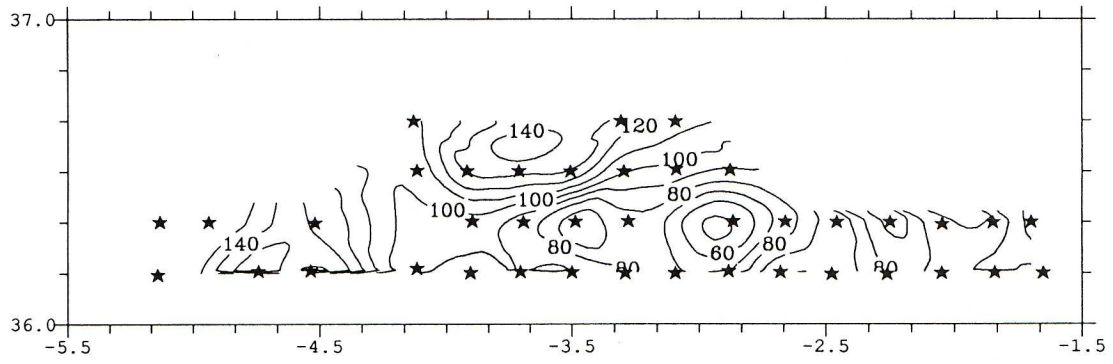

Figure 13. Depth of 14.5 °C isotherm from AXBT data.

Acknowledgments. This work would not have been possible without the expertise of all the people onboard the R/V *García del Cid*, especially J. Font, J. Salat, M. Manríquez, and A. Castellón (ICM). We gratefully also acknowledge the cooperation of the 801 Squadron of Search and Rescue, based in Palma de Mallorca, from the Ministerio de Defensa, who operated the aircraft. W. Wright (NASA) and P. E. La Violette (MSURC) were essential in the collection of the AXBT data. We thank R. Arnone and P. E. La Violette for processing the satellite images and for useful discussions and editing of the manuscript. We are also particularly thankful to A. Folkard and P. Davies (The University of Dundee) for useful discussion on the temporal variability from SST. Partial support for this study was obtained trough E.C. Euromodel project, MAST programme (MAS2-CT93-0066) and CICYT, AMB93-1046-CE. One of the authors (A.V.) acknowledges a PFPI grant from the CICYT.

References

Arnone, R. A., D. A. Wiesenburg, and K. D. Saunders, The origin and characteristics of the Algerian Current, *J. Geophys. Res., 95*(C2), 1587-1598, 1990.

Davies, P. A., A. M. Folkard, and G. C. d'Hières, Remote sensing observations of filament formation along the Almeria-Oran front, *Ann. Geophys., 11*, 419-430, 1993.

Donde Va? Group, ¿Donde Va? An oceanographic experiment in the Alboran Sea, The oceanographic report, *Eos Trans. AGU, 65*(36), 682-683, 1984.

Gascard, J. C., and C. Richez, Water masses and circulation in the western Alboran Sea and in the strait of Gibraltar, *Progr. in Oceanogr., 15*, 157-216, 1985.

Heburn, G. W., and P. E. La Violette, Variations in the structure of the anticyclonic gyres found in the Alboran Sea, *J. Geophys. Res., 95*(C2), 1599-1613, 1990.

Lanoix, F., Projet Alboran, Etude hydrologique et dynamique de la Mer d'Alboran, *Tech. Rep. 66*, 39 pp., 32 figures, NATO, Brussels, 1974.

La Violette, P. E., The Western Mediterranean Circulation Experiment (WMCE): Introduction, *J. Geophys. Res., 95*(C2), 1511-1514, 1990.

La Violette, P. E. (Ed.), *Seasonal and Interannual Variability in the Western Mediterranean, Coastal Estuarine Stud.*, vol. 46, 373 pp., AGU, Washinton, D.C., 1994.

McClain, C. R., G. Fu, M. Darzi, and J. Firestone, PC-SeaPack User's Guide Version 4.0, *NASA Tech. Memo. TM 104557*, 280 pp., 1992.

Perkins, H., T. Kinder, and P. E. La Violette, The Atlantic inflow in the Western Alboran Sea, *J. Phys. Oceanogr., 20*, 242-263, 1990.

Perkins, H., and P. Pistek, Circulation in the Algerian Basin during June 1986, *J. Geophys. Res., 95*(C2), 1577-1585, 1990.

Tintoré, J., P.E. La Violette, I. Blade, and A. Cruzado, A study of an intense density front in the eastern Alborán Sea: The Almería-Oran Front, *J. Phys. Oceanogr., 18*, 1384-1397, 1988.

Tintoré, J., D. Gomis, S. Alonso, and G. Parrilla, Mesoscale dynamics and vertical motion in the Alborán Sea, *J. Phys. Oceanogr., 21*, 811-823, 1991.

Viúdez, A., J. Tintoré, and R. L. Haney, Circulation in the Alboran Sea as determined by quasi-syjnoptic hydrographic observations. Part 1. Three-dimensional structure of the two anticyclonic gyres. *J. Phys. Oceanogr.*, in press, 1995.

Wang, D. P., The strait surface outflow, *J. Geophys. Res., 92*(C10), 10,807-10,825, 1987.

A. Víudez, Departament de Física, Universitat de les Illes Balears, 07071 Palma de Mallorca, Spain. (e-mail: DFSAVL4@ps.uib.es)

J. Tintoré, Department of Meteorology, Naval Postgraduate School, Monterey, CA 93943.

(Received November 30, 1993; revised July 6, 1994; accepted October 17, 1994.)